

Development Processes of the Tropical Pacific Meridional Mode

WU Shu^{*1,2} (武 术), WU Lixin¹ (吴立新), LIU Qinyu¹ (刘秦玉), and Shang-Ping XIE³

¹Physical Oceanography Laboratory, Ocean University of China, Qingdao 266100

²Center for Climatic Research, University of Wisconsin-Madison, Madison, WI, USA

³International Pacific Research Center and Department of Meteorology,
University of Hawaii, Honolulu, USA

(Received 21 April 2008; revised 26 April 2009)

ABSTRACT

Mechanisms for the spatio-temporal development of the Tropical Pacific Meridional Mode (TPMM) are investigated using a coupled ocean-atmosphere model and observations. In both observations and the model, this meridional mode displays decadal variations and is most pronounced in spring and early summer. The model simulation suggests that once SST anomalies in the subtropical northeastern Pacific are initiated, say by northeasterly trade wind variability, perturbations evolve into a meridional dipole in 2–3 months. A wind-evaporative-SST feedback causes a southwestward propagation of initial subtropical SST anomalies, while anomalous equatorial upwelling helps form the southern lobe of the meridional dipole. The TPMM development is a fast process (a few months) and depends on the seasonal cycle.

Key words: Tropical Pacific Meridional Mode, wind-evaporative-SST feedback, oceanic upwelling, decadal variation, seasonal phase lock

Citation: Wu, S., L. X. Wu, Q. Y. Liu, and S.-P. Xie, 2010: Development processes of the Tropical Pacific Meridional Mode. *Adv. Atmos. Sci.*, **27**(1), 95–99, doi: 10.1007/s00376-009-8067-x.

1. Introduction

ENSO is the dominant mode of the tropical Pacific ocean-atmosphere system, exerting profound impacts on the global climate (Klein et al., 1999; Alexander et al., 2002). The dynamics and prediction of ENSO have been extensively studied in recent decades (e.g., Wang and Picaut, 2004). Recent observational studies also suggest that there is an additional mode in the eastern tropical Pacific, with a center of SST anomalies north of the equator which couples to changes of the northeasterly trade winds and shifts of ITCZ (Fig. 1a). This mode is referred to as the Tropical Pacific Meridional Mode (TPMM), and is analogous to the tropical Atlantic meridional mode (Chiang and Vimont, 2004; CV04 hereafter). As a trigger for the TPMM, extratropical atmospheric variability can cause SST anomalies in the subtropical northeastern Pacific by varying the northeasterly trade winds and surface evaporation

(Vimont et al., 2001, 2003; Wu et al., 2007; Chang et al., 2007). It is unclear, however, how these subtropical SST anomalies can develop into the TPMM, with substantial tropical SST anomalies including a cold lobe in the equatorial eastern Pacific (Fig. 1a).

The present study tests the hypothesis that atmospheric-forced SST anomalies in the subtropics can develop subsequently into a meridional dipole with cooling near the equator, using an initial-value problem approach with a coupled model that simulates major features of the observed meridional mode when running freely. We will investigate the mechanisms for the spatial-temporal development of the TPMM. Section 2 describes the observational data and the model used in this study. Section 3 compares the TPMMs in the model simulation and observations. Section 4 presents the results from the initial value problem and studies the ocean-atmosphere interaction related to the formation of the meridional mode. Section 5 contains a

*Corresponding author: WU Shu, swu33@wisc.edu

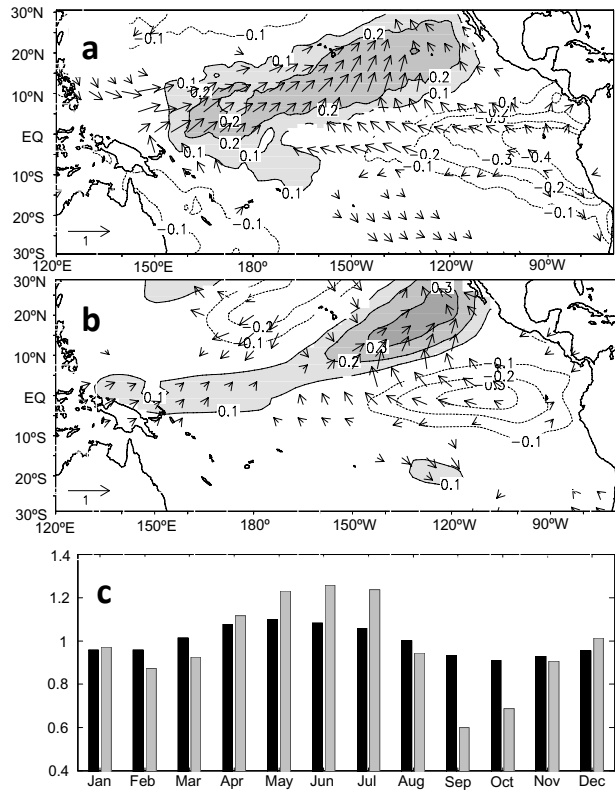


Fig. 1. Tropical Pacific meridional mode as represented by regression of SST (contours in $^{\circ}\text{C}$) and surface wind velocity (in m s^{-1}) against the normalized expansion coefficient of the relevant MCA mode in (a) observations (b) the model simulation. Only values that exceed the 95% confidence level are plotted. (c) Standard deviation of SST expansion coefficients in obsevations (black bars) and the model (grey).

summary and further discussion.

2. Observations and model

We use the HadISST dataset on a 1° grid for SST and the NCEP reanalysis on a 2.5° grid for the 1000 hPa wind velocity from January 1948 to December 2002. The Fast Ocean-Atmosphere Model (FOAM; Jacob, 1997; <http://www-unix.mcs.anl.gov/foam/>) is used, which has a tropical climatology typical of state-of-the-art climate models (Davey et al., 2002) and produces a reasonable ENSO (Liu et al., 2000). The atmospheric model has R15 resolution with 18 vertical levels, and the ocean model is solved on a 1.4° (lat) $\times 2.8^{\circ}$ (lon) grid with 32 vertical levels.

The control run is integrated for 100 years. In analyzing observations and model simulations, we first calculate the monthly mean anomaly by removing the mean seasonal cycle, and then apply a 3-month run-

ning mean. We use the Maximum Covariance Analysis (MCA, also called singular value decomposition; Bretherton et al., 1992) to extract coupled modes of SST and wind variability.

3. Observed and model-simulated TPMM

In observations, the first MCA mode is ENSO, with SST anomalies centered on the equator and changes in the easterly trade winds in the eastern tropical Pacific (not shown). The second MCA mode (Fig. 1a) is a meridional SST dipole, with a northeast-oriented lobe extending from the California coast to the central equatorial Pacific, and a lobe on or slightly south of the equator with the opposite polarity. This SST dipole with warm (cold) anomalies north (south) of the equator is associated with a reduction (enhancement) of the northeasterly (southeasterly) trade winds and anomalous southerly cross-equatorial winds, forming a C-shaped pattern as observed in the tropical Atlantic. This meridional mode is detected as the second mode in an EOF analysis for SST, accounting for 9% of the total SST variance.

The TPMM exhibits temporal variations distinct from ENSO. In observations, the ratio of SST variance between decadal (> 8 years) and interannual (2–7 years) timescales is 0.4 for the ENSO mode and 1.1 for the TPMM, respectively. Thus, the TPMM tends to be dominated by decadal variability and ENSO by interannual variability. Furthermore, the TPMM shows a seasonal phase locking pattern which is different from ENSO, with the strongest amplitudes in May–June (Fig. 1c). By contrast, the SST variance peaks in early winter for the ENSO mode (not shown). The TPMM as shown here is similar to that in CV04 but the southern lobe appears more robust in our analysis. This slight difference is perhaps due to the differences in observational data and the statistical method for removing ENSO. CV04 removes ENSO by subtracting a linear least-square fit to a cold tongue index while we do so by MCA mode decomposition.

In the control simulation, the first and third MCA modes of SST and surface winds in the tropical Pacific are ENSO (not shown) and the TPMM (Fig. 1b), respectively. The simulated TPMM resembles observations, with a meridional SST dipole, coupled with an anomalous C-shaped wind pattern. Compared to observations, the southern lobe of the simulated TPMM is somewhat shifted to the west away from the coast, while the northern lobe has weaker amplitudes in the central equatorial Pacific. In the model, TPMM appears as the second EOF mode for SST and accounts for about 9% of the total variance, the same as in observations. The modeled TPMM displays substan-

tial decadal variability (not shown) and a distinctive seasonal phase locking (Fig. 1c). The model TPMM peaks in June-July, lagging the observations by one month.

4. Sensitivity experiment

The TPMM explains a small fraction of total SST variance in the tropical Pacific ($\sim 9\%$ in both observations and the model). With a short observational record (<60 years), it is difficult to establish conclusively that the TPMM is not an artifact of statistical analyses. Since FOAM reproduces the statistical TPMM, we proceed to use it to test the hypothesis of Chiang and Vimont (2004) that the TPMM is a physical mode triggered by extratropical atmospheric variability. We adopt an initial-value problem approach and conduct an ensemble experiment initialized on May 31 with subtropical mixed layer temperature anomalies in the northeast subtropical Pacific. The initial SST anomalies are assumed to be induced by changes in the northeast trades associated with mid-latitude atmospheric variability such as from the North Pacific Oscillation (NPO; Vimont et al., 2001; CV04). NPO-induced SST anomalies can persist from DJF to JJA (see the composite results of CV04). The initial mixed-layer temperature anomaly has an oval-shape distribution in the horizontal with an area-averaged amplitude of 1°C , and is vertically uniform in the top 60m. The initial SST anomalies are much like Fig. 2a but confined to $10^{\circ}\text{--}20^{\circ}\text{N}$, $145^{\circ}\text{--}91^{\circ}\text{W}$. Thirty runs are conducted, each starting with May 31 initial conditions taken from a different year in the long control simulation. The ensemble difference between the sensitivity and control experiments is taken as the coupled response to the initial warming.

The initial warm anomaly in the northeastern subtropics decays rapidly (Fig. 2a) due to atmospheric damping associated with surface turbulent heat flux. The subtropical warming lowers *in-situ* atmospheric pressure and induces anomalous southwesterly winds the southern flank of the anomalous region. Superimposed on the prevailing easterlies, the anomalous southwesterlies reduce wind speed and surface evaporation, and cause a southwest displacement of the initial SST warming (Fig. 2b). To evaluate such an atmospheric feedback, we cast the Newtonian cooling associated with surface latent heat flux as $\varepsilon T'$ by linearizing the Clausius-Clapeyron equation (Xie, 1999). Here

$$\varepsilon = \frac{L \overline{Q}_E}{R \overline{T}^2}, \quad (1)$$

L is the latent heat of evaporation, R is the gas constant, Q_E and T are surface latent heat flux and SST,

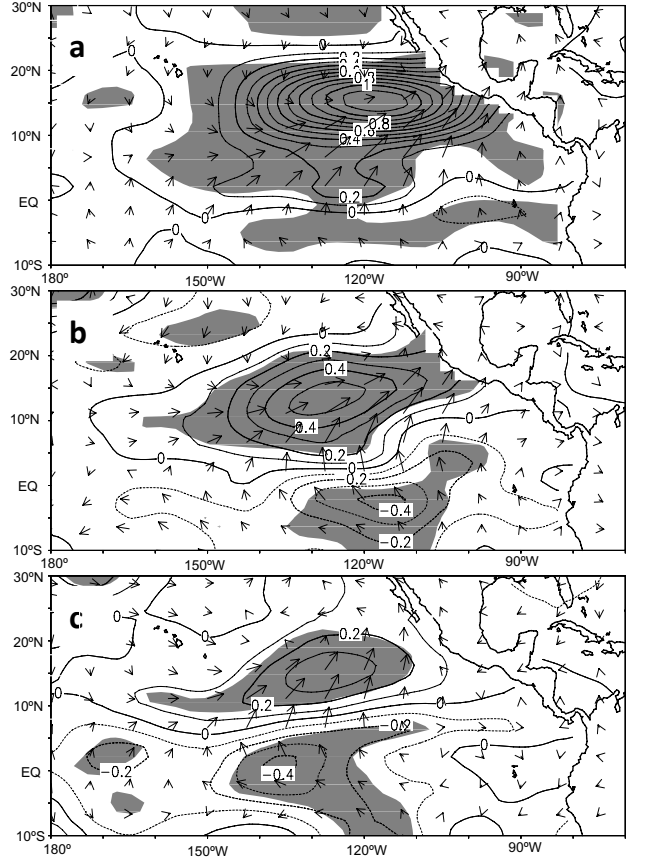


Fig. 2. SST (contours in $^{\circ}\text{C}$) and surface wind velocity (vectors in m s^{-1}) anomalies in the sensitivity experiment for (a) June, (b) July, and (c) August. SST anomalies exceed the 95% confidence level in shaded areas.

respectively, and the overbars and primes denote the values in and deviations from the control run. We then decompose surface latent heat flux into the Newtonian cooling and an atmospheric feedback term, as $Q'_E = \varepsilon T' + (Q'_E - \varepsilon T')$. The second term on the right hand side represents atmospheric feedback, say due to changes in wind speed. Figure 3 shows this atmospheric feedback term in latent heat flux. Positive feedback generally coincides with westerly wind anomalies, especially during June (Fig. 3a), indicating the importance of wind-induced evaporation.

Precipitation increases over the subtropical warm SST anomaly, and wind anomalies at 250 hPa are anticyclonic (not shown), opposite to surface cyclonic winds. The baroclinic atmospheric Rossby wave response to the subtropical SST warming—the anomalous southwesterlies and associated decrease in evaporation at the sea surface—is displaced southwest of the initial warming north of the equator. As a result, the subtropical SST warming displays a tendency to extend southwestward. On and to the south of the equator, the subtropical SST warming intensifies the

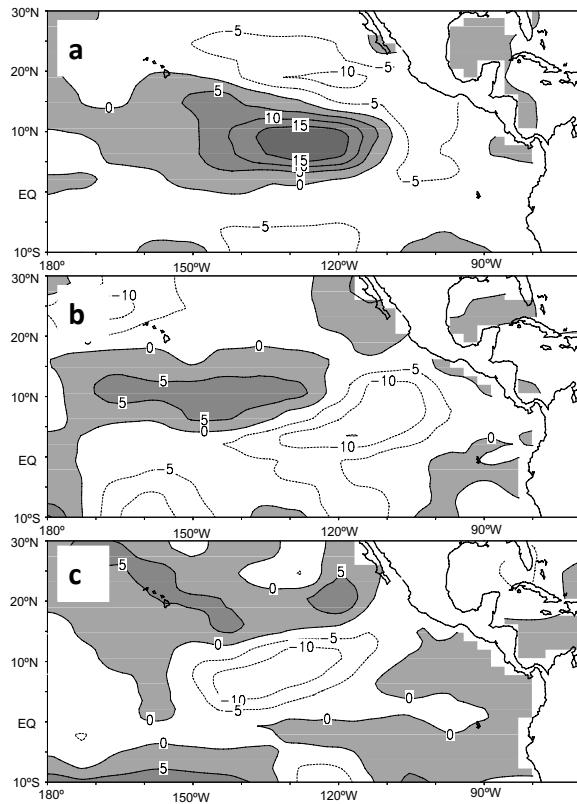


Fig. 3. Same as Fig. 2 but for latent heat flux minus the Newtonian cooling (W m^{-2}). Positive values are shaded and represent the ocean gaining heat.

prevailing southeasterly trade winds and surface evaporation (Figs. 2a–b and 3a–b), helping cool the SST there. This coupled response is consistent with the wind-evaporative-SST (WES) feedback mechanism identified for the tropical Atlantic meridional mode (Chang et al., 1997; Xie, 1999).

Shortly after the subtropical warming is introduced, negative SST anomalies begin to develop on and slightly south of the equator, growing to amplitudes comparable to the northern warming during July and August (Fig. 2). The meridional dipole induced by the subtropical warming (Figs. 2b, c) resembles TPMM in the control simulation and observations. A heat budget analysis (not shown) indicates that intensified upwelling is the main cause of the equatorial cooling. In July, the anomalous southeasterlies increase the upwelling on and slightly south of the equator (Fig. 4b), and indeed, the maximum SST cooling is displaced south of the equator (Fig. 2b). Areas of equatorial cooling, once formed, display a tendency to move westward, along with the maxima of the southerly cross-equatorial wind and the upwelling anomalies (Figs. 2–4).

After August, the SST dipole begins to decay because of the shift in the climatological wind. From

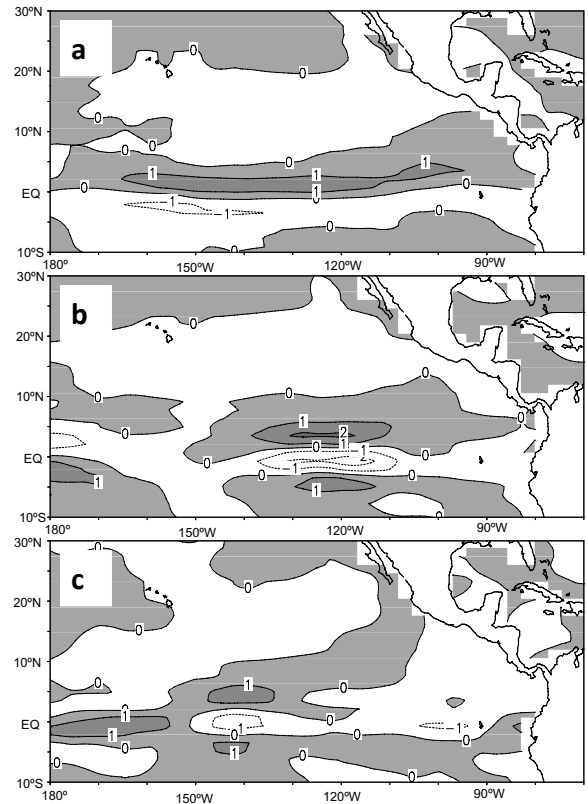


Fig. 4. Same as Fig. 2 but for vertical velocity (10^{-6} m s^{-1} ; positive downward).

June to September, the ITCZ continues its northward migration, and the climatological winds turn to southerly between the ITCZ and the equator. Superimposed on these climatological southerlies, the southwesternerly wind anomalies intensify surface evaporation and act to dampen the original SST warming. This effect of shifting the climatological wind is reflected in the northward shift of the nodal line of the SST dipole; the WES feedback turns negative between the ITCZ and the equator (Okajima et al., 2003).

A parallel ensemble experiment with negative initial SST anomalies in the subtropical northeastern Pacific yields similar results except for a sign difference. In another experiment with SST anomalies placed in the TPMM's southern lobe in the equatorial eastern Pacific, the model develops a Bjerknes mode with westward propagation along the equator. There tend to be SST anomalies of the opposite sign north of the equator but the amplitudes are small.

5. Conclusions and discussion

We have used a coupled model to investigate the mechanisms for the development of the TPMM in late spring and early summer. The model TPMM in the control run resembles observations in both spatial

structure and seasonal phase lock, with April–July as the preferred season for development. In the initial-value problem, an SST warming in the subtropical northeastern Pacific quickly develops into a TPMM-like meridional dipole, with the cool pole on the equator. The WES feedback induces a tendency for the initial subtropical warming to extend southwestward and reach the central Pacific while intensified upwelling appears to be the main cause of the equatorial cooling. The SST dipole begins to decay in late summer because the climatological winds are southerly and the WES feedback turns negative between the equator and northerly ITCZ. These results support the CV04 hypothesis that the TPMM is a physical mode triggered by subtropical wind variability associated with the North Pacific Oscillation.

The results from our initial value problem suggest that the TPMM can indeed develop during spring to summer, but this window of TPMM development does not extend into fall. This raises a question of why the TPMM prefers decadal timescales, if such a preference for timescales can be established from observations. Chang et al. (2007) suggest that TPMM often triggers El Niño in the subsequent summer. Since ENSO affects mid-latitude atmospheric variability, there is a possibility of tropical-extratropical interaction via the TPMM. Our coupled model also shows a tendency for El Niño to follow TPMM and that off-equatorial waves seem to play an important role in initializing ENSO (Wu, 2008). We are currently investigating why TPMM and ENSO occur in sequence and the implications for the interaction between the tropics and mid-latitudes via TPMM.

Acknowledgements. This work is supported by National Natural Science Foundation of China (40788002, 40676010, 40830106), and Japan Agency for Marine-Earth Science and Technology. This work is also supported by the ZhuFeng and Luka Projects of Ocean University of China (OUC) with funding from the Chinese Ministry of Education. Discussions with Zhengyu LIU, Ping CHANG, John CHIANG and Li ZHANG were helpful. All the simulations were carried at the OUC Ocean Data and Simulation Center. IPRC/SOEST publication #609/7745.

REFERENCES

- Alexander, M. A., I. Blade, M. Newman, J. R. Lanzante, N. C. Lau, and J. D. Scott, 2002: The atmospheric bridge: The influence of ENSO teleconnections on air-sea interaction over the global oceans. *J. Climate*, **15**, 2205–2231.
- Bretherton, C. S., C. Smith, and J. M. Wallace, 1992: An Intercomparison of Methods for Finding Coupled Patterns in Climate Data. *J. Climate*, **5**, 541–560.
- Chang, P., L. Ji, and H. Li, 1997: A decadal climate variation in the tropical Atlantic Ocean from thermodynamic air-sea interactions. *Nature*, **385**, 516–518.
- Chang, P., L. Zhang, R. Saravanan, D. J. Vimont, J. C. H. Chiang, L. Ji, H. Seidel, and M. K. Tippett, 2007: Pacific meridional mode and El Niño-Southern Oscillation. *Geophys. Res. Lett.*, **34**, L16608, doi: 10.1029/2007GL030302.
- Chiang, J. C. H., and D. J. Vimont, 2004: Analogous Pacific and Atlantic Meridional Modes of tropical atmosphere-ocean variability. *J. Climate*, **17**, 4143–4158.
- Davey, M., and Coauthors, 2002: STOIC: A study of coupled model climatology and variability in tropical ocean regions. *Climate Dyn.*, **18**, 403–420.
- Jacob, R. L., 1997: Low frequency variability in a simulated atmosphere ocean system. Ph.D. dissertation, University of Wisconsin-Madison, 155pp.
- Klein, S. A., B. J. Soden, and N. C. Lau, 1999: Remote sea surface temperature variations during ENSO: Evidence for a tropical atmospheric bridge. *J. Climate*, **12**, 917–932.
- Liu, Z., J. Kutzbach, and L. Wu, 2000: Modeling climate shift of El Niño variability in the Holocene. *Geophys. Res. Lett.*, **27**, 2265–2268.
- Okajima, H., S.-P. Xie, and A. Numaguti, 2003: Inter-hemispheric coherence of tropical climate variability: Effect of the climatological ITCZ. *J. Meteor. Soc. Japan*, **81**, 1371–1386.
- Vimont, D. J., D. S. Battisti, and A. C. Hirst, 2001: Footprinting: A seasonal connection between the tropics and mid-latitudes. *Geophys. Res. Lett.*, **28**, doi: 10.1029/2001GL013435.
- Vimont, D. J., J. M. Wallace, and D. S. Battisti, 2003: The seasonal footprinting mechanism in the Pacific: Implications for ENSO. *J. Climate*, **6**, 2668–2675.
- Wang, C., and J. Picaut, 2004: Understanding ENSO physics—A review. *Geophysical Monograph*, **147**, AGU, Washington D. C., 1–19.
- Wu, L., Z. Y. Liu, C., Li, and Y. Sun, 2007: Extratropical control of recent tropical Pacific decadal climate variability: A relay teleconnection. *Climate Dyn.*, **28**, 99–112.
- Wu, S., 2008: The main modes of local ocean-atmosphere interaction in north Pacific and its impacts on tropical Pacific. Ph.D dissertation, Ocean University of China, 143pp.
- Xie, S.-P., 1999: A dynamic ocean-atmosphere model of the tropical Atlantic decadal variability. *J. Climate*, **12**, 64–70.